Intelligent Monitoring on the Basis of a UAV for Assessing and Predicting the Condition of Objects with Complex Relief

Ainakulov Zh.Zh., Makarenko N.G., and Paltashev T.T.

***Abstract*—**This paper presents the practical experience of using an unmanned aerial vehicle (UAV) for accurate mapping of complex terrain. The use of aerial stereoscopic techniques with subsequent application of digital photogrammetry techniques is described. The obtained information on the area of the probed area, the boundaries of the cadaster is given. And also, intellectual monitoring of the given terrain, estimation, and prediction of the state of objects with a complex relief was carried out. The system of remote sensing based on UAV, its characteristics, such as economic efficiency, operation features, and estimation of the accuracy of flight over the geometry of the flight trajectory, is considered. The results of data processing using digital photogrammetry methods are obtained: the structure of motion algorithms and the geographic information system (GIS) for visualization, where the system makes it possible to obtain images with spatial resolution less than 10 cm, to determine the area of the site, to evaluate individual complex objects such as dumps, excavations or burial mounds, and also to make a topography of the investigated territories. The results of the study obtained by processing 3D models of mounds are presented. The technical characteristics of operated UAV with complexes with artificial intelligence are considered in detail.

***Keywords*—**artificial intelligence, assessing, complex objects, GIS, prediction, UAV.

I. Introduction

At present, the remote sensing industry is widely used in the geo-information market of Kazakhstan to support agriculture, forestry, and mining. In general, all applications or orders are based on aerial photographs. This is due to some reasons, such as the cost of production and the limited state of the infrastructure of the relief. Unfortunately, many remote sensing industries, like mine monitoring, do not have a platform for providing images on their own. In addition, some applications, such as monitoring the complex structure of objects taken from high-resolution satellite images, do not provide the required quality. One of the advantages of aerial photography compared with satellite imagery is the ability to monitor each individual object, if these objects have a complex structure.

Compared to satellite imagery, greater efficiency in obtaining the result is provided by the technical capabilities of modern UAV complexes (photo equipment, navigation, control and communication systems), which provide higher resolution (5 cm per pixel), as well as minimal dependence on weather conditions [1].

II. Assessment and Prediction of the Condition of Objects with Complex Relief

When creating a 3D-model of objects, the use of laser scanning technology can be most effective. When photographing large-sized complex objects (over 1 km2.), Dumps, pits, burial mounds and other objects, the labor costs for scanning and processing ground-based data increase in a geometrical progression [2].

To create a 3D-model of complex objects with significant dimensions, the technology of aviation stereo filming with the subsequent application of digital photogrammetry is used. At the same time, the accuracy of a 3D model depends on the shooting height and resolution of aerial imaging equipment [3]. Aviation stereo technology, followed by the use of digital photogrammetry methods, is based on observations and responds to changes within the area being filmed. It relies on new technologies such as imaging and information processing technologies. In addition, this technology makes it possible to more accurately determine the location of objects and their volumes in the relief using aerial photography.

Fig. 1 presents the archaeological complex “Boraldai Saki barrows”, Saki period (VI-III century BC). Consists of 47 large barrows. Sizes of barrows with a diameter of 80-150 m. and a height of 10-14 m.

The system consists of an antenna, a gyro platform, a digital camera, and data processing results using digital photogrammetry methods: the structure of motion algorithms and an open GIS source for visualization. This system has the ability to produce images with a spatial resolution of <10 cm, measure the area of the site, evaluate individual objects, such as mounds, as well as the topography of the studied areas.

Zh. Zh. Ainakulov is with the al-Farabi Kazakh National University, 71 al-Farabi Ave., Almaty, 050040, Republic of Kazakhstan (phone: +77014000401, e-mail: jaras1987@mail.ru).

N. G. Makarenko is with Institute of Information and Computational Technologies of MES RK, 125 Pushkin str., Almaty, 050010, Republic of Kazakhstan. (e-mail: ng-makar@mail.ru).

T.T. Paltashev is with the University of Information Technologies, Mechanics and Optics, St. Petersburg, 199034, Russian Federation (e-mail: timpal@mail.npu.edu).

Fig.1: Boraldai Saki Barrows

The main products of the system are *Agisoft PhotoScan* and *Photomod*. The average geometric accuracy can be obtained up to 3 pixels or the equivalent of submeter accuracy, including production time can be achieved in 50-52 hours. An orthophoto image can provide a visual interpretation, such as the structure of individual objects, the density of the location and the terrain with an accuracy of 3-6 pixels or 0.5-2.5 m.

Around the mounds are fences, funeral rings, altars. The need for a thorough study of the entire territory of the burial ground was the basis for aerial photography of the territory.

The use of aerial imaging systems using elements of artificial intelligence based on UAVs make it possible to accurately determine the planned coordinates, which is an important indicator when conducting cartographic works, when creating an orthophotomap and 3D elevation models, as well as optimizing the quality of the objects created and minimizing risks [4].

Fig.2: Orthophotomap

Good accuracy of the information in the process of managing aerial photographs allows instant monitoring of the state of the terrain (for example, every week or every few days). The mapping of the topography of the terrain and boundaries, as well as the analysis of the relief and volumetric calculation of a complex object, relief elements, are necessary for accurate measurement of parameters such as height, diameter, and slope of the terrain [5].

The survey was carried out for selected areas using elements of artificial intelligence based on UAVs. Digital images were created on a NEX-5N digital camera, with a resolution of 4912x3264, processing was carried out in the environment of *Agisoft PhotoScan*. The installation of digital orthophotoplans was carried out in the software product *Photomod*. Transformed images were sewn into a common mosaic. The stitching lines of the images were chosen with overlapping 80% [6]. Alignment of the photo tone was performed automatically. The accuracy of the orthophotomaps was checked by control points, which were determined in characteristic places of the relief with photogrammetric concentration of the reference network and not used in the transformation process. For each orthophotoplan, at least 5 points were determined at different heights. The maximum deviations of the position of these points on orthophotoplans from the calculated one did not exceed the tolerance - 0.45 m. [7].

Fig.3: 3D Elevation Model

Fig. 4 presents the initial points that are highlighted in blue. These control points indicate the latch position of the camera. Clearly highlights the camera positions and image overlap.

Aerial photographs were taken using a NEX-5N camera, with a resolution of 4912x3264, with a focal length of 24 mm.

Initial data:

- Total images: 91;
- Flight altitude: 61 m;
- Shooting resolution: 1.44 cm/pix;
- Coverage area: 0.0443 km²;
- Shooting positions: 91;
- Tie points: 101,193;
- Projections: 291.265;
- Error: 1.56 pixels.

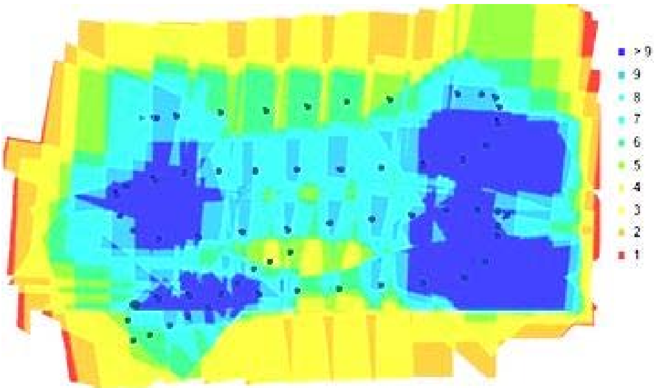

Fig.4: Positions of the Camera Latch and Image Overlap

III. Camera Calibration

91 images were taken from the camera.

The obtained aerial photographs of the area are processed automatically. One of the most common processing tasks is to automatically determine the overlap area and alignment of individual images (image stitching).

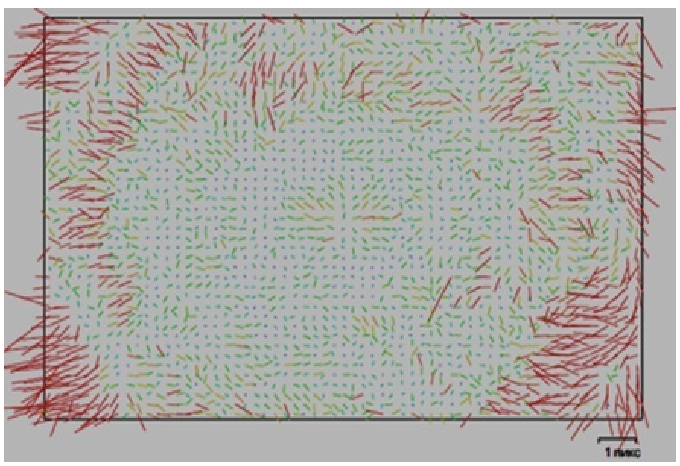

Fig.5: Failure to Tie Points for NEX-5N

Table 1. Camera Indicators

Resolution	Focal length	Pixel size	Calibration
4912x3264	24 mm.	4.98x4.98 microns	Yes
Type:	frame by frame	**F:**	3903.44
Cx	-67.176	**B1:**	0.720422
Cy	57.0259	**B2:**	0.0465502
K1	-0.0419109	**P1:**	-0.00259134
K2	0.0539813	**P2:**	0.00455211
K3	-0.0707309	**P3:**	-1.17503
K4	0.030755	**P4:**	1.41258

Information obtained as a result of image stitching, the overlapping area and the relative position of the photographs can be used to build accurate site plans, to analyze any events or changes in the terrain. Such tasks are related to the tasks of computer vision, which is currently one of the most rapidly developing branches of information technology. In this task, we will use the methods of extracting images from the SFM structure (Structure from motion), highlighting the structure in motion and simultaneously localizing and matching the construction of SLAM (Simultaneous localization and mapping) maps.

When performing aerial photography, a number of simplifications are allowed, which allow increasing the speed of data processing. On the other hand, there are problems associated with poor conditioning of some subtasks and a large number of errors in the solutions obtained by classical methods [8].

In this paper, two approaches are proposed, methods for extracting images from the SFM structure, highlighting the structure in motion and simultaneously localizing and comparing the construction of SLAM maps, which allow speeding up the processing of data obtained from aerial photography, as well as the asymptotic estimate of the working time of these methods.

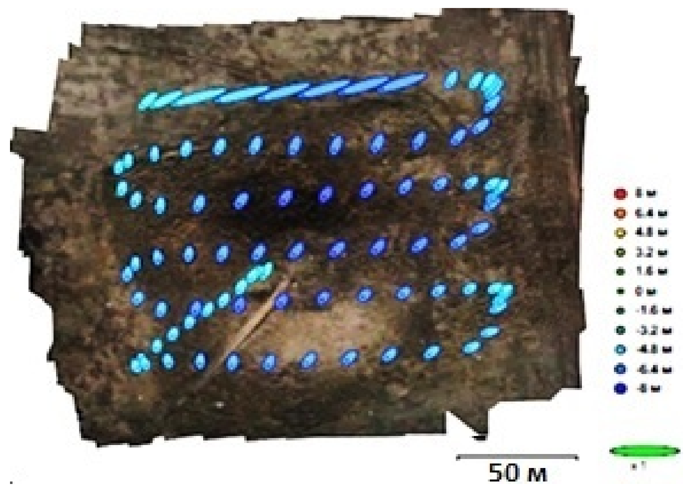

Fig.6: Shooting Positions and Error Estimation

Z error is displayed in the blue ellipse. Errors in the plan are displayed in the form of an ellipse. The calculated shooting positions are marked with a black point inside the blue figures, the deviation errors by coordinates are shown in Table 2 and Table 3.

Table 2. Coordinate Deviation Errors

X		У		Z		XУ		General error
1,6	-1,6	1,6	-1,6	3,2	-3,6	1,6	-1,6	1,6
1,8	-1,8	1,7	-1,62	3,1	-3,8	1,75	-1,71	3,2
2,2	-2,2	1,8	-1,63	3,6	-4,2	2	-1,915	4,65
2,3	-2,3	1,9	-1,64	4,8	-4,4	2,1	-1,97	5,4
4,5	-4,5	2	-1,7	5,2	-3,9	3,25	-3,1	5,7
5,5	-4,6	2,1	-1,72	5,6	-4,4	3,8	-3,16	5,8
6,8	-4,7	2,4	-1,74	5,8	-4,8	4,6	-3,22	5,9
0,9	-4,8	4,2	-1,75	5,9	-5,3	2,55	-3,275	6,7
7,2	-5	4,8	-2	6,7	-6,7	6	-3,5	7,2
7,8	-5,1	4,9	-4,2	6,9	-7,8	6,35	-4,65	7,8
7,6	-5,2	5,2	-4,3	7,2	-8,7	6,4	-4,75	7,86
7,5	-5,3	5,4	-5	8,2	-9,5	6,45	-5,15	7,95
7,9	-6,2	5,6	-5,1	8,6	-7,8	6,75	-5,65	7,99
8	-6,1	5,8	-5,2	9	-8	6,9	-5,65	8

Table 3. Average Camera Position Error

Error, X (m)	Error, Y (m)	Error, Z (m)	Error, XY (m)	General Error (m)
5,1641	3,531	6,255	4,28	5,26

In Fig. 7, the positions of the control points are indicated in red, and the control points are highlighted in yellow, where 01; 02; 03; 04; 05; 06 are reference points.

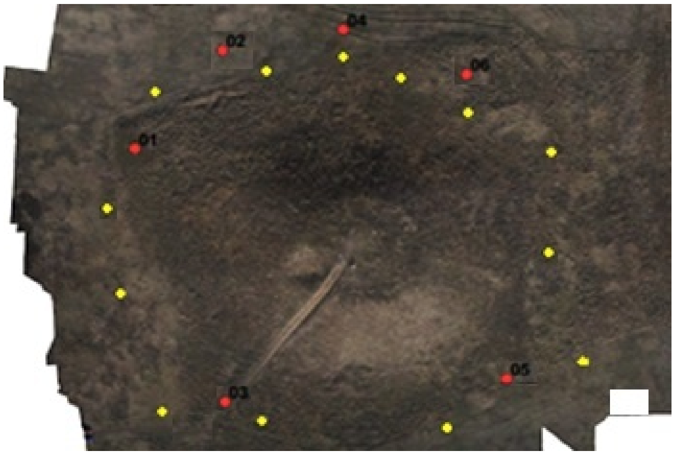

Fig.7: Positions of Reference Points

The standard deviation is the root of the variance, and is calculated by the formula:

$$S = \sqrt{\frac{\sum_{i=1}^{n}(x-\bar{x})^2}{n}}; \quad (1)$$

Table 4 presents the standard deviation S over the reference points, respectively, along with the coordinates X, Y, Z, where the total error is 19.12 cm.

Table 4. Standard Deviation S on Reference Points

Error, Sx (cm)	Error, Sy (cm)	Error, Sz (cm)	Error, Sxy (cm)	General Error (cm)	Photo (pix)
9.18614	16.5288	2.07874	18.91	19.1239	2.667

Table 5 shows the deviation of the X, Y, Z coordinates of reference points, where the total deviation was 19.02 cm.

Table 5. Reference Points

Name	Error, X (cm)	Error, Y (cm)	Error, Z (cm)	General Error (cm)	Photo (pix)
03	-1.66794	-5.08534	2.45898	5.88976	4.774 (6)
04	5.3696	0.490129	-0.134663	5.39361	0.645 (6)
05	0.94732	6.35043	-1.90732	6.69801	0.834 (3)
02	-19.1376	-25.8512	3.13648	32.3167	0.951 (5)
01	7.13126	29.3518	-1.6143	30.2488	1.537 (9)
06	7.52976	- 6.55534	1.94446	10.1711	3.464 (8)
General	9.18614	16.5288	2.07874	19.0239	2.667

From an orthophotomap, which contain contour information, you can measure the area of the plot and the diameter of the dome, while the 3D model or digital height of the model product can be analyzed and evaluated to obtain information related to the structure of complex objects, such as a blade (pit), surface reliefs of mounds, etc [9].

The digital terrain model that was obtained as a result of image stitching, the overlap area (80%) and the relative position of the photos are shown in Fig. 8. A point cloud obtained as a result of aerial photography processing can be used to build an accurate model of a complex object, as well as to analyze any events or changes occurring in the area [10].

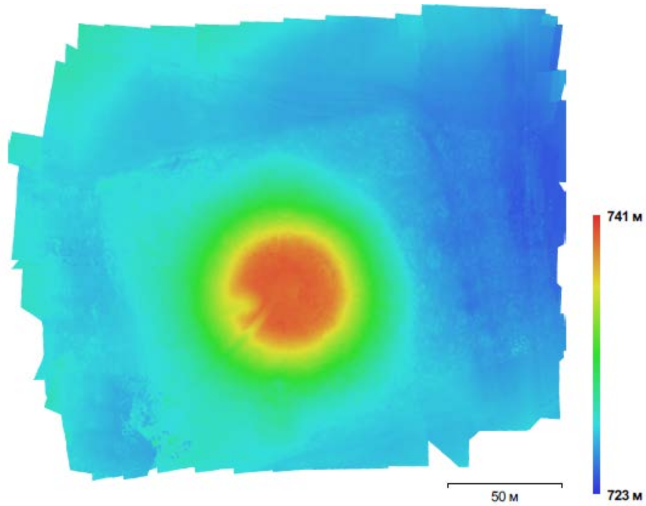

Fig.8: Calculated Digital Terrain Model

The digital model of a complex object was obtained as a result of processing aerial photographs with a resolution of 2.89 cm/pix and a density of points: 1.2e + 03 points / m². On the digital terrain model, blue is shaded with a height of 723m. above sea level, this is the basis of the mound, and the red height of the mound is 741 m., then the real height of the mound is 18 m.

Table 6. Processing Parameters

Main	
Images: 91	Aligned images: 91
Markers: 6	Coordinate system: WGS 84 / UTM zone 43N (EPSG:32643)
Point cloud	
The number of points: 101,193 of 107,576	Reprojection error: 0.402228 (1.56268 pixels)
Max. reprojection error: 6.53615 (17.4621 pixels)	Effective overlap: 2.95872
The average size of points:	4.84778 pix
Alignment options	
Accuracy: Very high	Preselection pairs: Binding
Max. number of points: 40,000	Max. number of projections: 4,000
Filter by mask: No	Adaptive refinement of camera model: Yes
Time to search for matches: 13 minutes 5 seconds	Leveling time: 1 minute 5 seconds
Optimization options	
Parameters	f, b1, b2, cx, cy, k1-k4, p1-p4
Optimization time	6 seconds
Dense point cloud	
Points:	66,445,969
Reconstruction parameters	
Quality: High	Filtration Depth maps: Soft
Calculation time of depth maps: 1 hour 47 minutes	Calculation time of a dense cloud: 35 minutes 0 s.
Model	
Polygons 13,225,901	Texture 4,096x4,096, uint8
Vertices	6,618,110

Reconstruction parameters	
Surface Type: Height Map	Interpolation: Enabled
Baseline:	Dense Point Cloud
Quality: High	Filtration Depth maps: Soft
Number of polygons 13,289,193	Processing time: 3 minutes 57 seconds
Texturing options	
Parameterization Mode:	Orthophoto
Blend Mode: Mosaic	Texture Size 4,096x4,096
Enable color correction: Yes	Enable hole filling: Yes
Time parameterization: 2 minutes 34 seconds	Texture mixing time: 10 minutes 53 seconds
Tile model. Reconstruction parameters	
Baseline: Thick cloud	Tile size: 4096
Processing time: 3 hours 51 minutes	Heights Map
Size 12,221x11,238	Coordinate system WGS 84 / UTM zone 43N (EPSG::32643)
Reconstruction parameters	Baseline: Thick cloud
Interpolation Enabled	Processing time 4 minutes 50 seconds
Orthophoto Plan	Size 16.809x14.955
Coordinate system WGS 84 / UTM zone 43N (EPSG::32643)	Channels 3, uint8
Blending Mode:	Mosaic
Reconstruction parameters	
Surface: Height Map	Include color correction: No
Processing time:	3 minutes 55 seconds
Program	
Version 1.2.6 build 2834	Platform: Windows 64 bit

IV. Conclusion

This article presents a practical experience of using the platform of an unmanned aerial vehicle (UAV), which performs remote sensing of the earth to create an accurate mapping of the terrain of a given area. On the UAV platform, a gyro platform carrying a digital camera is used to perform aerial photographs. Thus, the developed method can be used to find the relationship between the structural parameters of individual objects (Height, Density), which can be measured by this system with a potential supply of solutions. The main products of the system are an orthophoto map and a digital elevation model (cloud of 3D points) with an accuracy of 2-pixel errors for the horizontal position and 5-pixel error for the vertical. The coordinates of the control points verify the accuracy of the orthophotoplans, they were selected from certain places of relief that were not used in the transformation process. For each photomap, at least 5 points with different elevations have been selected. The limit value of the deviation of the coordinates of control points on orthophotoplans from the calculated ones does not exceed the permissible value by 0.45 m.

Acknowledgment

The authors express their deep appreciation to the Committee of Science, Ministry of Education and Science of the Republic of Kazakhstan, for the funding of the research.

References

[1] Makarov V.A., Bondarenko D.A., Makarov I.V., Shrainer K.A., Perunov A.A., Trukhanov E.V., Bespilotnye letatel'nye apparaty dlya resheniya zadach marksheiderii i monitoringa otkrytykh gornykh rabot (Unmanned aerial vehicles for surveying and monitoring of open pit mining), OOO NPP “AVAKS-GeoServis”. Available at: http://uav-siberia.com/en/news/bespilotnye-letatelnye-apparaty-dlya-resheniya-zadach-marksheyderii-i-monitoringa-otkrytykh-gornykh-rabot/

[2] Beloshapkin M. A., Avtomaticheskii tsifrovoi aerofotos"emochnyi kompleks Photolite (Digital automatic aerial survey complex “Photolite”), Shestoi Mezhdunarodnyi seminar pol'zovatelei sistemy PHOTOMOD (VI International PHOTOMOD User Conference), Becici, Montenegro, 19-22 September 2006, Book of Abstracts, 44 p.

[3] Khan N.Y., Imran A.S., Ali N, Distance and color invariant automatic license plate recognition system Emerging Technologies, 2007, ICET 2007, International Conference, pp. 232-237.

[4] Klasing K., Wollherr D., Buss M, A clustering method for online segmentation of 3d laser data, Proc, ICRA, 2008, pp. 4043-4048.

[5] Sveshnikova N.V., Yurin D.V., Otsenka pogreshnostei vosstanovleniya trekhmernykh stsen algoritmami faktorizatsii (Estimation of errors in the reconstruction of three-dimensional scenes by factorization algorithms), 2006, pp. 28-33. Available at: http://www.graphicon.ru/html/2006/proceedings/papers/fr09_32_Sveshnikova_Yurin.pdf

[6] Sin'kova M.G., Ispol'zovanie tsifrovoi aeros"emki i sozdanie ortofotoplanov po materialam s"emki tsifrovoi aeros"emochnoi kamery ADS-40 (The use of digital aerial photography and the creation of orthophotos on the materials of the shooting of a digital aerial camera ADS-40), VII Mezhdunarodnaya nauchno-tekhnicheskaya konferentsiya "Ot snimka k karte: tsifrovye fotogrammetricheskie tekhnologii" (The VII-th International Scientific and Technical Conference "From imagery to map: digital photogrammetric technologies"), September 17-20, 2007, Bulgaria, p. 41. Available at: http://www.racurs.ru/download/conf/Bulgaria2007/Presentations/Sinkova.pdf

[7] Instruktsiya po fotogrammetricheskim rabotam (Instruction on photogrammetric works), KIShINEU, 2010. Available at: http://geoportal.md/ru/default/uploads/index/id/48

[8] Karpov D.P., Rodikov D.E., Sshivka izobrazhenii, poluchennykh v rezul'tate aerofotos"emki (Cross-linking of images obtained as a result of aerial photography), ITMO University, 2012, pp. 3-6. Available at: http://is.ifmo.ru/projects/2012/karpov/description.pdf

[9] Ainakulov Zh.Zh., Makarenko N.G., Paltashev T.T. Experience of modeling mining landscapes by using methods of intelligent monitoring. The journal “Current problems in remote sensing of the Earth from space”, 2018. Volume 15. №7. P. 43-50. Available at:: http://d33.infospace.ru/d33_conf/sb2018t7/43-50.pdf

[10] Tailakov O.V., Korovin D.S., Osobennosti fotogrammetricheskoi obrabotki aerofotosnimkov otkrytogo ugol'nogo sklada pri ispol'zovanii bespilotnykh letatel'nykh apparatov (Features of photogrammetric processing of aerial photographs of an open coal warehouse using unmanned aerial vehicles), Vestnik of Kuzbass State Technical University, 2016, pp. 1-4.